



## WCCE11 - 11th WORLD CONGRESS OF CHEMICAL ENGINEERING

IACCHE - XXX INTERAMERICAN CONGRESS OF CHEMICAL ENGINEERING  
CAIQ2023 - XI ARGENTINIAN CONGRESS OF CHEMICAL ENGINEERING  
CIBIQ2023 - II IBEROAMERICAN CONGRESS OF CHEMICAL ENGINEERING

Buenos Aires - Argentina - June 4-8, 2023

"The global chemical engineering working for a better future world"

### Iron nanoparticles based nanofluids for *in situ* environmental remediation

**Crespi, J.**<sup>1,2\*</sup>, **Binetti Basterrechea, G.F.**<sup>2</sup>, **Finoli, A.S.**<sup>2</sup>, **Montesinos, V.N.**<sup>2,3</sup>,  
**Quici, N.**<sup>2,3</sup>

<sup>1</sup>Instituto Sabato, Universidad Nacional de San Martín - Comisión Nacional de Energía Atómica, Av. Gral. Paz 1499, B1650KNA, San Martín, Buenos Aires, Argentina.

<sup>2</sup>Centro de Tecnologías Químicas, Departamento de Ingeniería Química, Facultad Regional Buenos Aires, Universidad Tecnológica Nacional, Medrano 951, C1179AAJ, Ciudad Autónoma de Buenos Aires, Argentina.

<sup>3</sup>División Química de la Remediación Ambiental, Centro Atómico Constituyentes, Comisión Nacional de Energía Atómica, CONICET, Av. Gral. Paz 1499, San Martín, Buenos Aires, Argentina.

\* [julicrespi@gmail.com](mailto:julicrespi@gmail.com)

#### ABSTRACT

The injection of nanoscale zerovalent iron particles (nZVI) suspensions in the ground is a technology employed for *in situ* water and soil remediation. Due to its nature, nZVI forming these nanofluids (NFs), tend to agglomerate, but this can be overcome by polyelectrolyte coatings, that also improve their mobility.

In this work, stabilization of nZVI with carboxymethylcellulose (CMC) was studied. NFs prepared with CMC (CMC-NSTAR) were compared with non-stabilized NFs (b-NSTAR). First, the stabilization efficiency was evaluated by the analysis of the nanoparticles sedimentation rate. Then, the mobility of stabilized and non-stabilized NFs was studied in columns filled with porous media at laboratory and pilot scale. Finally, NFs reactivity for the removal of aqueous Cr(VI) was tested in batch and columns experiments. In the column experiments, a porous media bed was loaded with NSTAR and then a Cr(VI) solution was injected upwards.

CMC-NSTAR showed good mobility at both scales being successfully eluted from the porous media. In the case of b-NSTAR, the accumulation of nanoparticles in the bottom of the column was observed and elution was not achieved. Using b-NSTAR as reactive barrier, a total removal of 15.5 mg Cr(VI)/g Fe was achieved. Better removal rates were found in batch experiments (22.8 mg Cr(VI)/g Fe). Reactivity experiments in batch with CMC-NSTAR showed 39.9 mg Cr(VI)/g Fe removal.

In conclusion, the NF was proved to have good transport properties and Cr(VI) removal capacity.

**Keywords:** *in situ*, zerovalent iron nanoparticles, Cr(VI), stable nanofluids

#### 1. INTRODUCTION

Nanoscale zerovalent iron (nZVI) is a useful technology for remediation of polluted water. nZVI can remove a variety of pollutants by redox reactions or adsorption (Quici et al. 2018). For *in situ* groundwater treatment, suspensions of nZVI, also named nanofluids (NFs) are injected in the ground for water and soil remediation. The main obstacle is the nZVI tendency to agglomerate, which hinders their injection and prevents further transport. To address this disadvantage, the use of different polyelectrolytes as coating is an efficient solution that leads to the nZVI stabilization and improves their mobility in porous media (Priyadarshini et al. 2022). Different polyelectrolytes had been proved to stabilize nZVI, such as carboxymethylcellulose (CMC), xanthan gum, guar gum, starch, between others. Chromium is a major water and soil pollutant present as  $\text{HCrO}_4^-$  and  $\text{Cr}^{3+}$  species and introduced in the environment by several industrial processes.  $\text{HCrO}_4^-$  is carcinogenic (Zhitkovich 2011) and its removal

by nZVI is mainly based in the adsorption in the surface of the nanoparticles (NPs) or its reduction to  $\text{Cr}^{3+}$  that imposes a minor health risk as it is an essential nutrient. The Cr(VI) removal process by nZVI has been well described making it suitable system to use as probe for iron based NPs reactivity and removal capacities (Montesinos et al. 2014).

In this work, stabilization of commercial nZVI with CMC was studied. First, stabilization efficiency was evaluated by the analysis of the NPs sedimentation rate. Then, the mobility of stabilized and non-stabilized NFs was studied in porous media packed bed columns at laboratory and pilot scale. Finally, NFs reactivity for the removal of aqueous Cr(VI) was tested in batch and columns experiments.

## 2. MATERIALS AND METHODS

### 2.1 Nanofluids preparation and stabilization

Commercial nZVI (NANO FER STAR, hereafter NSTAR) were provided by NANO IRON s.r.o. as a powder with a nominal particle size of 50 nm and 65-80% of elemental iron (Nano Iron, s.r.o.). CMC, provided by Sigma-Aldrich, was used as stabilizer. Milli-Q quality water (resistivity  $18 \text{ M}\Omega \text{ cm}^{-1}$ ) was used in laboratory scale experiments, obtained with a OSMOION water purifying equipment (APEMA), and purged using nitrogen or argon gas for deoxygenation. Tap water was used for pilot scale tests.

A post-synthesis approach was used for the preparation of stabilized nanofluids. For that purpose, a highly concentrated NSTAR suspension was prepared by weighting NSTAR and adding Milli-Q water, and then mixed for 2 minutes with a Pro Scientific homogenizer. Two dilution steps were carried out by adding water and then ultrasonicated in an ultrasonic bath (Cleanson). Ultimately, equal parts of NSTAR suspension and CMC solution were mixed in an orbital shaker (Vicking) for one hour. Two stabilized NFs were prepared: CMC10-NSTAR, with  $10 \text{ g L}^{-1}$  of CMC and  $1 \text{ g L}^{-1}$  of Fe(total), and CMC5-0.5NSTAR, with  $5 \text{ g L}^{-1}$  of CMC and  $0.5 \text{ g L}^{-1}$  of Fe(total). Also, a non-stabilized nanofluid with  $1 \text{ g L}^{-1}$  of Fe(total), b-NSTAR, was prepared by following the same steps but without adding CMC (and adding Milli-Q water instead).

Stabilization was evaluated by sedimentation rate analysis of the nanoparticles in CMC10-NSTAR versus b-NSTAR. Both nanofluids were placed in closed flasks and settling was observed by taking pictures periodically.

### 2.2 Transport evaluation

Transport ability of NSTAR was studied at laboratory and pilot scale in sand packed columns. Figure 1 shows a scheme of the experimental setup. Briefly, a peristaltic pump (APEMA) was used to feed the nanofluid upwards through the porous media packed column. The nanofluids were kept under mechanical agitation to prevent the settling of the nanoparticles. Samples were taken periodically at the outlet to determine concentration of nanoparticles.

Silica sand used as porous media was previously treated with  $\text{H}_2\text{O}_2$ , successively washed with tap water and Milli-Q water, and finally dried at  $150 \text{ }^\circ\text{C}$ . Both columns were assembled by placing a filter at the bottom and then adding the sand slowly to ensure a compact packaging. Finally, a second filter was placed at the top of the porous bed to prevent sand losses. Filters were composed of glass wool, and gravel was also added for pilot experiments.

NaCl solutions were used as tracers to evaluate the characteristic retention time of the porous bed. The NaCl concentration at the outflow of the column was determined by measuring the conductivity of the solutions with a conductivity meter (Hach, SensION).

The transport tests were performed in two stages. First, the column was fed with the tested material. Then, the retained material in the column was eluted with water.

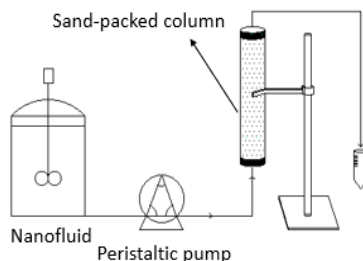


Figure 1. Experimental setup used to perform transport tests.

#### 2.2.1 Laboratory scale

NFs transport experiments at laboratory scale were performed using a glass column with an internal diameter of 4 cm and a 21 cm high sand bed. Laboratory tests were carried out using CMC10-NSTAR and b-NSTAR. The materials were pumped at a  $12 \text{ mL min}^{-1}$  flow rate. Samples were taken periodically at the exit of the column, and their turbidity was determined using a portable turbidimeter (Hach). The

turbidity was taken as a measure of the iron nanoparticles concentration. The breakthrough curves of iron were plotted with the obtained turbidity measurements.

### 2.2.2 Pilot scale

Pilot test experiments were conducted using CMC5-0.5NSTAR. An acrylic column of 50 cm length and 4 cm internal diameter was constructed to carry out the tests. A 46 cm high porous bed of sand was assembled. In this case, the flow rate was  $30 \text{ mL min}^{-1}$ , and the two-stage experiments were also performed. First, the NF was fed to column and samples were collected periodically at the exit, for the construction of the breakthrough curves. Then, the column was washed with tap water to study the elution of the previously retained iron material.

### 3.3 Reactivity evaluation

Removal of Cr(VI) was studied to evaluate NPs reactivity in different conditions. Cr(VI) solutions were prepared employing  $\text{K}_2\text{Cr}_2\text{O}_7$  (Mallinkrodt). Prior to each experiment, highly concentrated NSTAR suspensions were activated for 48 hours at room temperature before use.

Preliminary removal batch tests were conducted with CMC10-NSTAR, b-NSTAR and f-NSTAR (without any steps of dilution), at initial pH 3 (adjusted with  $\text{H}_2\text{SO}_4$ ) with a total volume 100 mL and an initial concentration of Cr(VI) of  $15.6 \text{ mg L}^{-1}$ . In these experiments, a Fe:Cr molar ratio (MR) of 10 was employed. Cr(VI) and nanofluids were mixed in an Erlenmeyer flask, and agitated in an orbital shaker (Vicking) for 60 minutes.

For the column experiments,  $1 \text{ g L}^{-1}$  b-NSTAR, non-stabilized nanofluids were prepared. The experimental set up used is depicted in Fig 1. The porous media was initially fed upwards with the suspension until a 0.5 g of NSTAR reactive barrier was formed. Afterwards, 200 mL of a  $100 \text{ mg L}^{-1}$  Cr(VI) solution was injected upwards through the reactive barrier, at  $6 \text{ mL min}^{-1}$  (approximately for 30 minutes). Finally, the column was fed with Milli-Q water, to elute the Cr(VI) possibly retained in the porous media. To compare these results, batch experiments with the same mass of Cr(VI) and nZVI were performed, by mixing 100 mL of  $200 \text{ mg L}^{-1}$  Cr(VI) solution and 100 mL of b-5NSTAR ( $5 \text{ g L}^{-1}$  of Fe(total)) in an Erlenmeyer flask (20 mg of Cr(VI) and 0.5 g of Fe(total)). The flask was agitated using an orbital shaker for 30 minutes at 200 rpm. At the end of the experiment, samples were centrifuged with an Eppendorf MiniSpin centrifuge at 13,000 rpm. The supernatant of each sample was used separately for Cr(VI) and Fe(total) determination. Final pH was measured with a portable pHmeter (Hach).

Fe(total) and Cr(VI) concentrations were measured spectrophotometrically with a Hewlett Packard Agilent 8453UV-Vis spectrophotometer. [Cr(VI)] was measured via the diphenylcarbazide colorimetric method by measuring the absorbance at 540 nm (ASTM 1992). [Fe(total)] was measured via the hydroquinone – *o*-phenanthroline colorimetric method by measuring the absorbance at 508 nm (Harvey et al. 1955).

## 3. RESULTS AND DISCUSSION

### 3.1 Stability evaluation

Stabilization was evaluated by sedimentation rate analysis of the nanoparticles in CMC10-NSTAR versus b-NSTAR placed in flasks. Figure 2 shows the photographs taken at different times, flask A containing CMC10-NSTAR and B, b-NSTAR. As Fig. 2 shows, at  $t = 5 \text{ min}$ , b-NSTAR starts to sediment, and at  $t = 45 \text{ min}$  sedimentation is almost completed. On the other hand, during this period, CMC10-NSTAR remains without any visible settling. Only after one day, sedimentation of CMC10-NSTAR is visible, and after 3 days appears to be completed.

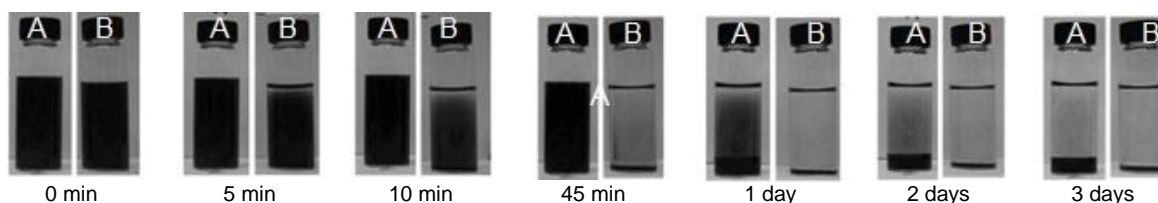


Figure 2. Photographs of CMC10-NSTAR (A) and b-NSTAR (B) at different times.

### 3.2 Transport evaluation

#### 3.2.1 Laboratory scale

Figure 3 shows the results of the transport experiments carried out at laboratory scale using stabilized CMC10-NSTAR and non-stabilized b-NSTAR, compared with the NaCl tracer curve. As it can be observed in Fig. 3 (a), b-NSTAR did not reach the outlet of the column; on the contrary, transportation of the nanoparticles was minimum and they were observed to accumulate at the bottom of the column.

On the other hand, CMC10-NSTAR showed good mobility: NPs reached high concentration at the exit of the column after 5 pore volumes, although the initial curve slope is lower than the tracer curve. This behavior could be explained by the major resistance to mass transfer that nanoparticles already reported in literature (He et al 2009). The maximum normalized concentration of NPs obtained was 0.8 at 8 pore volumes, value that slowly decreased with time. Possibly, NPs transport caused pore plugging in the sand packed column (Tiraferrri and Sethi 2009) hindering the NF transport. After the first stage, the elution of the retained materials was studied. As shown in Figure 3 (b), b-NSTAR could not be eluted, evidenced by the absence of iron in the column outlet. On the contrary, retained NPs were completely eluted by feeding the column with water in the experiment with CMC10-NSTAR. It was observed that the elution was not smooth as at 4 pore volumes a concentration 3 times higher than the initial was observed. This could be explained by an initial accumulation of NPs and an abrupt release of them in the elution.

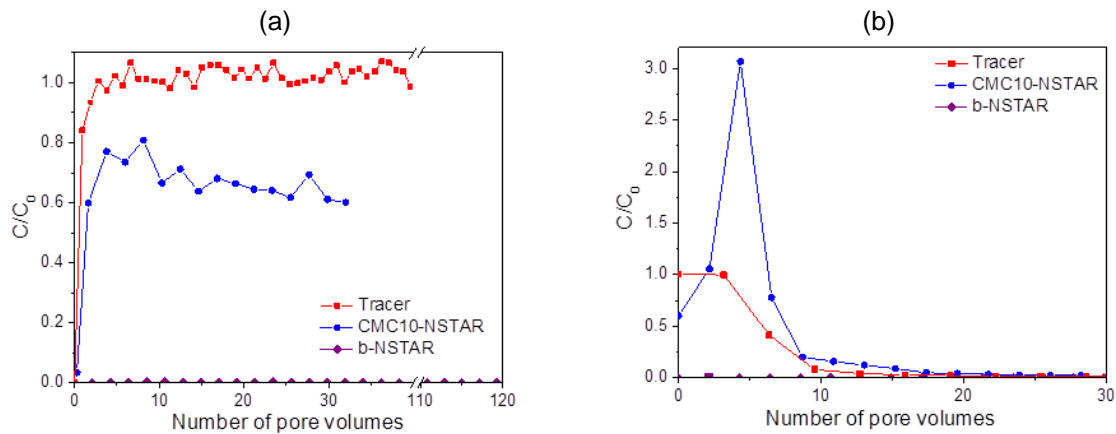


Figure 3. CMC10-NSTAR, b-NSTAR and tracer breakthrough curves at laboratory scale for (a) continuous feeding of material, and (b) elution with Milli-Q water.

### 3.2.2 Pilot scale

Figure 4 shows the results of experiments carried at pilot scale using CMC5-0.5NSTAR, compared with the tracer curve. As seen at laboratory scale, stabilized nanofluid showed good mobility although the curve slope is lower than the one corresponding to the tracer. NPs reached 50% of initial concentration at the exit of the column after feeding it with 5 pore volumes of nanofluid. It might be expected that after this maximum, the concentration decreases progressively, as it was seen at laboratory scale.

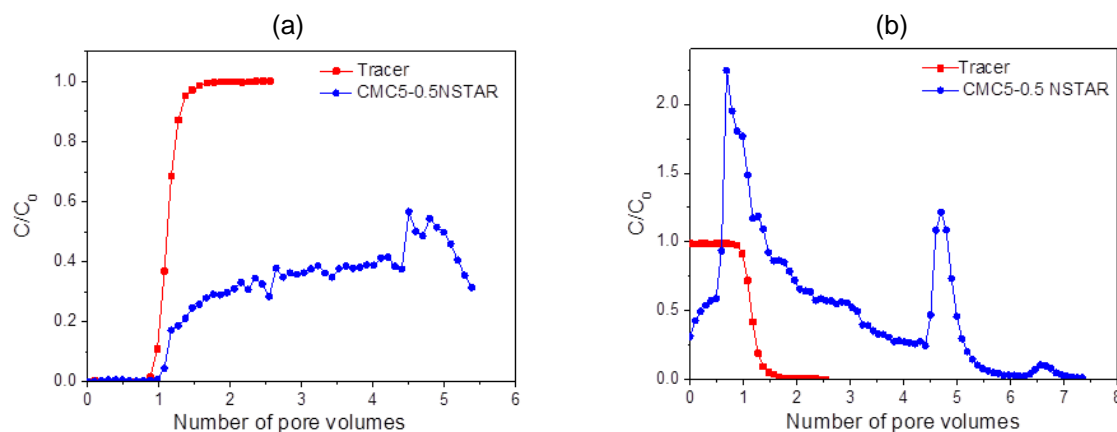


Figure 4. CMC5-0.5NSTAR and tracer breakthrough curves at laboratory scale for (a) continuous feeding of material, and (b) elution with Milli-Q water.

Figure 4 (b) shows the results of the elution of materials. Two points of high concentration were observed and a fast decline to zero concentration, when retained NPs were completely eluted.

As a partial conclusion, stabilized NFs showed good mobility in both scales. However, at laboratory scale (as the operational conditions and the preparation of the bed are easier to control) a higher normalized concentration of NPs was achieved at the exit of the column. Laboratory and pilot scale experimental results are not easy to compare. There are several differences in the operational conditions, one of them is the difference in flow velocity. Whereas laboratory tests were run at  $15.3 \text{ cm min}^{-1}$ , at pilot scale the velocity was  $3.18 \text{ cm min}^{-1}$ . Considering that NPs drag can be disadvantaged

with lower flow velocity (Raychoudhoury et al. 2014), only experiments at the same flow velocity should be compared. Additionally, although the same CMC:Fe mass ratio was used, the concentration of CMC in laboratory experiments was higher than pilot scale experiments, causing a higher viscosity which could prevent gravity sedimentation (Tosco y Sethi 2010). It is worth mentioning that same operational conditions in different scales are not easily achieved as challenges of experimental set up at larger scales are more difficult to overcome.

### 3.3 Reactivity evaluation

Cr(VI) removal was tested with different nanofluids to study their reactivity in different conditions. Preliminary batch tests, with a Fe:Cr MR = 10 and initial pH = 3, were performed. This initial pH was previously optimized for the Cr(VI) removal with free-in-suspension nZVI (Montesinos et al. 2014). Three nanofluids were tested: CMC10-NSTAR, b-NSTAR and f-NSTAR. In all cases, following the provider recommendations, the original NSTAR suspension was left in a closed flask for 48 hours at room temperature for activation (Nano Iron, s.r.o.). Both b-NSTAR and f-NSTAR were non-stabilized nanofluids, but the b-NSTAR suffered the steps of dilution described in section 2.1, while f-NSTAR were prepared as highly concentrated NSTAR suspension, activated, and then added to the Cr(VI) solution. In this conditions, 100% of initial Cr(VI) was removed with f-NSTAR in 30 minutes, while only around 36% was removed with b-NSTAR in 60 minutes, indicating a decreased reactivity after the nanofluid preparation process. With CMC10-NSTAR, above 40% of the initial Cr(VI) was removed in 60 minutes, showing that the presence of CMC as stabilizing agent, could partially prevent the loss of reactivity of the nanoparticles. For better comparison, the amount of Cr(VI) removed was calculated as mg Cr(VI)/g Fe: 92.9 with f-NSTAR, 33.2 with b-NSTAR and 39.9 with CMC10-NSTAR.

After these results, column tests were performed. Since b-NSTAR showed poor mobility in porous media, as it could be seen in Figure 3, a permeable reactive barrier was created by pumping b-NSTAR onto a silica sand bed column. Elution of the material was not achieved after washing the column with Milli-Q water. On the other hand, Cr(VI) solution transport in silica sand was previously studied, obtaining a breakthrough curve that matches the one corresponding to NaCl (tracer). Also, the adsorption of Cr(VI) onto silica sand was studied in batch experiments and finding it negligible. Then, the column with the NSTAR barrier was fed with the solution of Cr(VI), and both Cr(VI) and Fe(total) were measured in the samples taken at the column outlet.

Figure 5 exhibits the Cr(VI) breakthrough curve in the presence of NSTAR barrier (Cr(VI) with reactive barrier) compared to the system in the absence of NPs (Cr(VI) without reactive barrier). As it can be observed in Fig. 5(a), in the absence of NSTAR barrier, the normalized concentration reached the value of 1 after 1.7 pore volumes (i.e., the outlet concentration rapidly matched the inlet concentration), showing no retention of Cr(VI) in the system. In the presence of the reactive barrier, the concentration at the outlet reaches a value close to the one injected at the inlet only after 25 pore volumes. Fig. 5(b) shows the Cr(VI) elution curves for both systems.

For the total curves (feeding + elution), the area under the curve allows to calculate the total mass of Cr(VI) found at the outlet of the column. After performing a mass balance, Cr(VI) retention in the bed due to the interaction with nZVI was evidenced leading to a total removal of Cr(VI) of 15.5 mg Cr(VI)/g Fe.

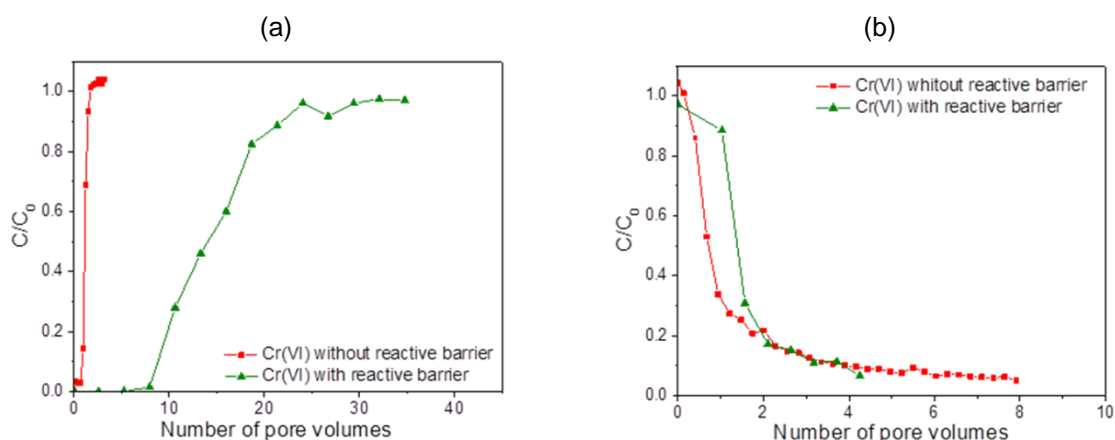


Figure 5. Cr(VI) breakthrough curves at laboratory scale with and without the presence of a NSTAR barrier at (a) continuous feeding of material, and (b) elution with Milli-Q water.

Batch tests in the same conditions as column tests (and with the same nanofluid) were performed simultaneously, achieving a total removal of 22.8 mg of Cr(VI)/g Fe (57% of the initial Cr(VI)). These results obtained present a divergence, despite trying to replicate the experimental conditions. One

possible explanation could be that for column experiment the nanofluid suffered one dilution step further, that could be affecting its reactivity.

For a better comparison, Table 1 shows all the results found with the tested nanofluids.

As it can be seen, the results for b-NSTAR in batch do not differ significantly from each other, even when in one case pH was not adjusted. Nevertheless, all of the experiments greatly differ from f-NSTAR, showing a high loss of reactivity due to the NFs preparation processes.

Though column experiments with CMC10-NSTAR are pending, batch reactivity experiments lead us to expect that the presence of CMC will allow to partially prevent the reactivity reduction.

Table 1. Comparison between test conditions and results for the removal of Cr(VI) with different nanofluids.

Nanofluid tested	Experiment	pH <sub>0</sub>	[Cr(VI)] <sub>0</sub>	MR Fe:Cr	Cr(VI) removed (mg Cr(VI)/g Fe)
f-NSTAR	Batch	3 (adjusted)	15.6 mg L <sup>-1</sup>	10	92.9 in 30 min (100%)
b-NSTAR	Batch	3 (adjusted)	15.6 mg L <sup>-1</sup>	10	33.2 in 60 min (36%)
CMC10-NSTAR	Batch	3 (adjusted)	15.6 mg L <sup>-1</sup>	10	39.9 in 60 min (43%)
b-NSTAR	Batch	4.5 (not adjusted)	100 mg L <sup>-1</sup>	23	22.8 in 30 min (43%)
b-NSTAR	Column	4.5 (not adjusted)	100 mg L <sup>-1</sup>	23	15.5 in 30 min (35%)

#### 4. CONCLUSIONS

In conclusion, NFs prepared using CMC as stabilizer were proved to have good transport properties at both laboratory and pilot scale, and Cr(VI) removal capacity in batch tests. Due to its poor mobility, non-stabilized NFs can be used as permeable reactive barrier in porous media, but with decreased reactivity. To simulate more realistic applications, Cr(VI) removal experiments with CMC-NSTAR in columns should be performed.

#### References

- ASTM D1687 (1992). Standard Test Methods for Chromium in Water.
- Harvey Jr. A. E., Smart J. A. Amis E. S. (1955). Simultaneous spectrophotometric determination of iron(II) and total iron with 1,10-phenanthroline. *Analytical Chemistry*, 27(1), 26–9.
- He F., Zhang M., Qian T., Zhao D. (2009). Transport of carboxymethyl cellulose stabilized iron nanoparticles in porous media: Column experiments and modeling. *Journal of Colloid and Interface Science*, 334, 96-102.
- Montesinos V., Quici N., Halac E., Leyva A., Custo G., Bengio S., Zampieri G., Litter M. (2014). Highly efficient removal of Cr(VI) from water with nanoparticulated zerovalent iron: Understanding the Fe(III)–Cr(III) passive outer layer structure. *Chemical Engineering Journal*, 244, 569-575.
- Nano Iron, s.r.o. Manual for preparation of an aqueous suspension from dry stabilized iron powder NANOFER STAR. <https://nanoiron.cz/getattachment/7aa3e8c5-5701-4a47-b05c-b91f87279aae/NANOFER-STAR-processing-activation-manual.aspx>. Last accessed: 10.27.2022.
- Priyadarshini A., Kumar Sahoo P., Ghosal A., Kumar Sahoo N. (2022). Stabilization of zero-valent iron for wastewater treatment: Challenges and future prospective. *Materials Today: Proceedings*, 67, 1073–9.
- Quici N., Meichtry M., Montesinos V.N. Use of Nanoparticulated Iron Materials for Chromium, Arsenic, and Uranium Removal from Water. In: Litter MI, Quici N, Meichtry M. *Iron nanomaterials for Water and Soil Treatment*, Singapore: Pan Stanford Publishing; 2018, p. 177-200.
- Raychoudhury T., Tufenkji N., Ghoshal S. (2014). Straining of polyelectrolyte-stabilized nanoscale zero valent iron particles during transport through granular porous media. *Water Research*, 50, 80-9.
- Tiraferri A., Sethi R. (2009). Enhanced transport of zerovalent iron nanoparticles in saturated porous media by guar gum. *Journal of Nanoparticle Research*, 11, 635-45.
- Tosco T., Sethi R. (2010). Transport of Non-Newtonian Suspensions of Highly Concentrated Micro- And Nanoscale Iron Particles in Porous Media: A Modeling Approach. *Environmental Science and Technology*, 44, 9062-8.
- Yu Q., Guo J., Muhammad Y., Li Q., Lu Z., Yun J., Liang Y. (2020). Mechanisms of enhanced hexavalent chromium removal from groundwater by sodium carboxymethyl cellulose stabilized zerovalent iron nanoparticles. *Journal of Environmental Management*, 276, 111245.
- Zhitkovich A. (2011). Chromium in drinking water: Sources, metabolism, and cancer risks. *Chem. Res. Toxicol.*, 24, 1617-29.